

# A MULTICOMPONENT REACTIVE TRANSPORT MODEL INCORPORATING KINETICALLY CONTROLLED PYRITE OXIDATION<sup>1</sup>

Murray D. Wunderly<sup>2</sup>, David W. Blowes<sup>3</sup>, Emil O. Frind<sup>4</sup>, Carol J. Ptacek<sup>5</sup>, Tom A. Al<sup>6</sup>

**Abstract:** A numerical model (MINTOX) has been developed to simulate the diffusion of oxygen into mine-tailings impoundments and the oxidation of pyrite, coupled with the subsequent reactive transport of the oxidation products through the tailings impoundment. A shrinking-core oxidation model and a finite-element numerical method are used to simulate the transport of oxygen and oxidation of pyrite grains. The rate of pyrite oxidation is assumed to be limited by the transport of oxygen to the reaction site. The oxidation products released by pyrite oxidation are transported along with the pore water and react with other aqueous components and the solid tailings. The advective and dispersive transport of the aqueous components is accomplished using a finite-element transport code. The equilibrium chemical composition of the pore water is calculated nodally during each time step by a modified version of MINTEQA2. MINTOX can be used to assess the sensitivity of mine-tailings impoundments to the various hydrogeological and geochemical conditions. Effects of remedial measures such as the addition of moisture retaining covers or the addition of chemical additives to the tailings such as lime can be quantitatively modelled.

**Key Words:** Pyrite oxidation, oxygen diffusion, reactive transport, finite-element, acid-mine drainage.

## Introduction

Mathematical models have become important tools for predicting and assessing groundwater contamination problems. Typically, groundwater flow and chemistry are modelled separately using different mathematical models, but, because groundwater undergoes physical and chemical changes simultaneously, it is advantageous to simultaneously couple these processes in a single model. Mine-tailings environments are an example where models which couple multiple processes may be valuable tools in assessing acid mine drainage problems. Groundwater flowing through the mine tailings undergoes extreme chemical variations, and the chemical interactions between the various minerals and aqueous components can be overwhelmingly complex. Geochemical reactions occurring within mine tailings include: aqueous speciation, acid-base, mineral precipitation/dissolution, ion exchange and redox reactions. When reaction rates between the aqueous components and the solid-phase minerals are rapid, the local equilibrium assumption (LEA) is accurate. The chemical species will be in a state of thermodynamic equilibrium, and an equilibrium mass-action approach to the geochemical modelling can be adopted.

---

<sup>1</sup>Paper presented at Sudbury '95, Conference on Mining and the Environment, Sudbury, Ontario, May 28th - June 1, 1995.

<sup>2</sup>Wunderly, M.D., Research Hydrogeologist, Waterloo Centre for Groundwater Research, University of Waterloo, Waterloo, Ontario, N2J 3G1.

<sup>3</sup>Blowes, D.W., Assistant Professor, Waterloo Centre for Groundwater Research.

<sup>4</sup>Frind, E.O., Professor, Waterloo Centre for Groundwater Research.

<sup>5</sup>Ptacek, C.J., Research Geochemist, Water Research Institute, Environment Canada, Canada Centre for Inland Waters, Burlington, Ontario, L7R 4A6.

<sup>6</sup>Al, T.A., Graduate Student, Waterloo Centre for Groundwater Research.

However, if the flow rates of the pore water are fast relative to the reaction rates, then a kinetic modelling approach must be used. An example where a kinetic approach must be adopted is the oxidation of pyrite within mine-tailings impoundments. These oxidation reactions may be rate limited by diffusion of oxygen into the tailings (1, 2) and may remain in disequilibrium for decades or longer. The oxidation of pyrite, and other sulfide minerals, within mine tailings impoundments is responsible for the high acidity and mobility of heavy metals which is observed.

A reactive transport model which incorporates kinetically controlled pyrite oxidation (MINTOX) has been developed. The model consists of three main modules: a finite-element transport model (PLUME2D), an equilibrium-geochemistry model (MINTEQA2), and an oxygen-diffusion and pyrite-oxidation model (PYROX). The first two of these modules were previously coupled by Walter et al. (3) into the reactive transport program MINTRAN. The third module PYROX was developed as a stand alone program to model oxygen diffusion and pyrite oxidation in mine-tailings environments. PYROX has been successfully coupled with MINTRAN. The resulting model, MINTOX, simulates diffusion of oxygen and the oxidation of pyrite as well as the subsequent reactive transport of the oxidation products.

### Oxygen Diffusion and Pyrite Oxidation

The diffusion of oxygen and pyrite oxidation occurring within mine-tailings impoundments are modelled as a two-stage process. The first stage considers the diffusion of oxygen into the pore space of the tailings from the atmosphere, and the second considers the diffusion of oxygen into the pyrite particles of the tailings through an oxidized shell forming around an unoxidized core. This two-stage process is shown graphically in Figure 1. As pyrite grains oxidize, the thickness of the oxidized coating increases, further inhibiting oxygen from reaching the unreacted core. Assuming that oxygen reaching the unreacted pyrite core of the particles reacts instantaneously, with the pyrite, the oxygen concentration at the boundary between the unreacted core and the oxidized coating will be zero. The concentration gradient between the outer surface of the particle and the unreacted core will continue to cause oxygen to diffuse into the particles until the unreacted core is completely oxidized, at which time the particle will no longer consume oxygen nor produce sulfate, iron, and acidity. Figure 2 shows the oxygen concentration gradient within a partially oxidized pyrite grain.

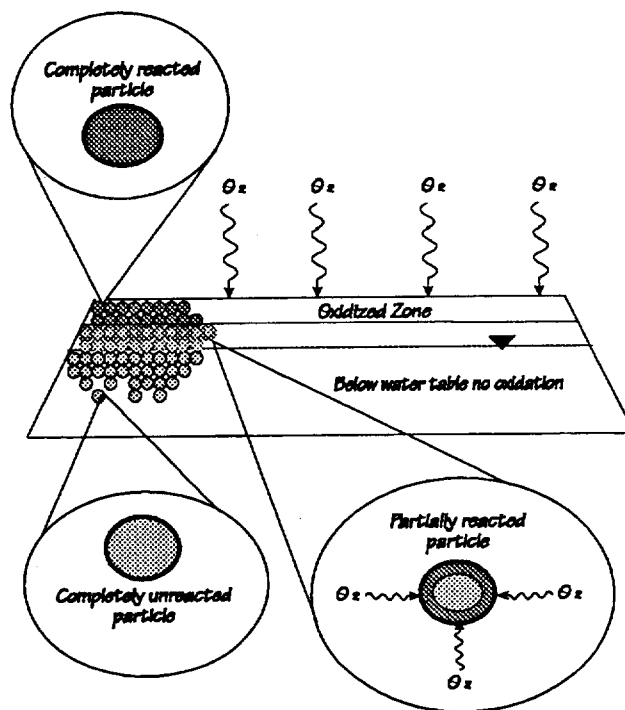


**Figure 1. Two-stage oxidation process in a tailings impoundment**

The diffusion of oxygen into tailings impoundments can be assumed to be a one-dimensional process because tailings are commonly spread laterally over hundreds to thousands of square meters, whereas the depth of the unsaturated zone where oxidation occurs is usually only a few meters. Oxygen diffuses from the surface, where the concentration of oxygen is equal to atmospheric, inward or down toward the water table, which constitutes a zero gradient boundary condition for the diffusion of oxygen.

The numerical model PYROX is based on the algorithm developed by Davis (4) and Davis et al. (5), who developed a finite-difference numerical model describing oxygen diffusion and pyrite oxidation in waste-rock dumps. The waste-rock model was not suitable for this application because it assumes a homogeneous medium, and the development of the mathematics results in equations which are dimensionless in time. Because the intent was to couple oxygen diffusion and pyrite oxidation to the existing program, MINTRAN, it was necessary to have the time variable as a dimensioned quantity. Also, variability of input parameters such as moisture content, pyrite content, bulk density, and porosity were desired. The variability of moisture content within mine tailings is particularly important because it may cause the bulk diffusion coefficient for oxygen within the tailings to vary by several orders of magnitude. The variable diffusion coefficient for oxygen in a porous medium can be calculated using equation 1 (6) based on the moisture content, porosity and temperature of the medium. The equations describing oxygen diffusion and pyrite oxidation developed by Davis (4), and Davis and Ritchie (1) were rederived with the shrinking core portion of the model on the mathematical development of Levenspiel (7). Equation 2 describes the bulk diffusion of oxygen into the tailings and the subsequent loss of oxygen to the pyrite grains. Equation 3 describes the rate at which the unreacted pyrite cores of the particles shrink. These two equations constitute a system of 2 equations and 2 unknowns, and thus a unique solution may be obtained.

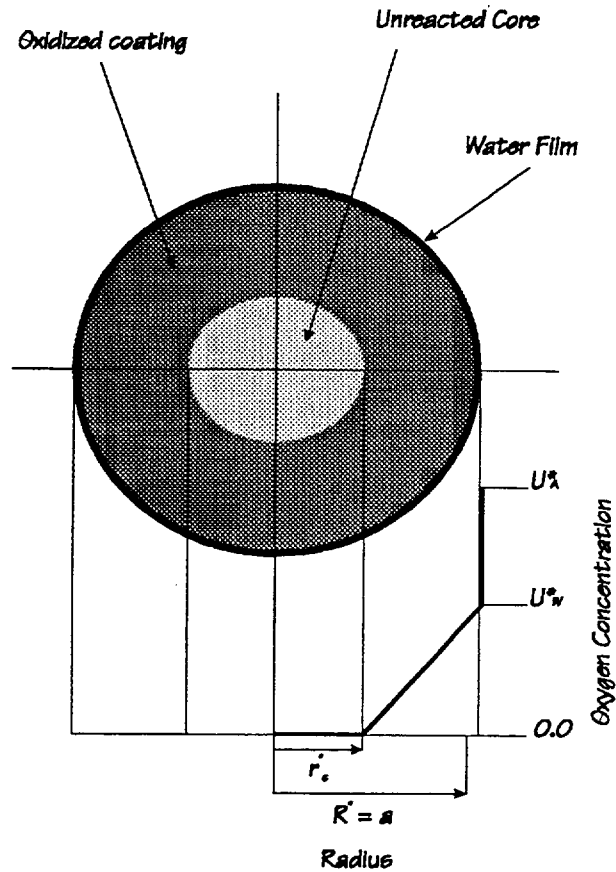


**Figure 2. Partially oxidized pyrite grain. Oxygen concentration gradient between surface of particle and unreacted core causes oxygen to diffuse into particle.**

$$D1(x) = 3.98 \times 10^{-9} \times \left[ \frac{apor(i) - 0.05}{0.95} \right]^{1.7} \times (Temp)^{1.5} \quad (1)$$

$$apor(x) \frac{\partial U_A(x,t)}{\partial t} = D1(x) \frac{\partial^2 U_A(x,t)}{L^2 \partial x^2} - \frac{3(1 - por(x))D2}{a^2} \left( \frac{r_c(x,t)}{1 - r_c(x,t)} \right) U_A(x,t) \times XHEN \quad (2)$$

$$\frac{dr_c(x,t)}{dt} = \frac{D2(1 - por(x))U_0}{\epsilon \rho_s(x) a^2} \left( \frac{r_c(x,t)}{r_c(x,t) - r_c(x,t)^2} \right) U_A(x,t) \times XHEN \quad (3)$$

where,

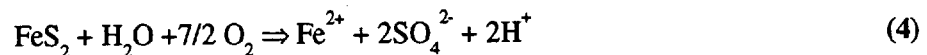
$apor(x)$	- is the air filled porosity of the tailings [ ]
$frac{sulf}(x)$	- fraction of sulfur in tailings [ ]
$por(x)$	- is the porosity of the tailings [ ]
$r_c(x,t)$	- is the radius of the reaction front within the particle or the radius of the unreacted core [m].
$D1(x)$	- is the diffusion coefficient for the porous media [ $m^2/s$ ].
$D2$	- is the diffusion coefficient for the oxidized rim [ $m^2/s$ ]. surrounding the unoxidized core of the particles [ $m^2/s$ ].
$R^*$	- is the unreacted radius of the particle [m].
$R_k$	- chemical source/sink term [mol/kg s].
$U_A^*(x,t)$	- is the oxygen concentration in the pore space [ $kg/m^3$ ].
$U_w^*(x,t)$	- is the concentration of oxygen in the film of water surrounding the particle [ $kg/m^3$ ].
$XHEN$	- is 1/(Henry's constant for oxygen).
$\epsilon$	- ratio of oxygen to sulfur consumed by pyrite [ ]
$\rho_s(x)$	- density of sulfur within tailings [ $kg/m^3$ ].

\* means the variable is not dimensionless. The same variable without \* is dimensionless.

Equation 2 is solved using the Galerkin finite-element method as opposed to a finite-difference method used by Davis et al. (5). The versatile nature of the finite-element method allows for spatially variable input parameters to be easily assigned. Equation 3 is solved using a Newton-Raphson technique, similar to that of Davis et al. (5). The algorithm used to solve these equations remains the same as that of Davis et al. (5). Equations 2 and 3 are solved iteratively until the concentration of oxygen in the pore space,  $U_A(x,t)$ , and the radius of the unreacted pyrite cores,  $r_c(x,t)$ , converge simultaneously.

### Pyrite Oxidation By-products

The oxidation of pyrite, which consumes oxygen and produces  $H^+$ ,  $SO_4^{2-}$ , and Fe(II), is shown in the following equation:



Because PYROX calculates the radius of the unreacted cores, the mass of pyrite consumed can be calculated. Using the mass of pyrite consumed and the stoichiometry of equation 4, the mass of sulfate, iron and acidity produced due to pyrite oxidation can be calculated.

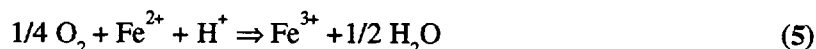
Neither analytical models nor numerical models capable of modelling heterogeneous systems were available to verify the PYROX model. Thus, the model could only be verified for a homogeneous system through comparison with results from the model of Davis et al. (5). The two models produced nearly identical results. PYROX was also tested using field data from Nickel Rim, Ontario (8). The tailings at Nickel Rim have been oxidizing for approximately 35 years. Moisture content data collected in 1991 by Johnson (8) was used as input data, along with the data shown in Table 1. The field data and modelled results for pore-space oxygen concentration and percentage of sulfur remaining in the tailings solids are shown in Figures 3 and 4, respectively. PYROX calculates the rate of contaminant production due to pyrite oxidation and may also be used to determine how long pyrite oxidation will continue. Although the rates and masses of oxidation products are calculated within PYROX, the fate of these oxidation products

remains unknown. Because we are ultimately concerned with the fate of the oxidation products, it is necessary to link the pyrite-oxidation process to the reactive transport processes which are occurring. Therefore, the numerical model PYROX was coupled with the reactive transport model MINTRAN. The resulting model MINTOX, thus simulates the oxidation of pyrite and the production of oxidation products as well as determining the fate of these oxidation products as they flow through the groundwater system and react with the tailings solids and other aqueous components in the pore water. PYROX operates only in the unsaturated zone with the water table acting as the lower boundary. MINTRAN operates in both the saturated and unsaturated zone with the surface of the tailings as the upper boundary, and the base of the tailings as the lower boundary.

**Table 1. Physical parameters used in Nickel Rim oxidation simulation**

Parameter	Value
D1	calculated from moisture content
D2	1.5 E-14 [m <sup>2</sup> /s]
Particle Radius	7.5 E-5 [m]
Porosity	0.415
Bulk Density	1550 [kg/m <sup>3</sup> ]
% Sulfur	4.5
Depth	1.0 [m]
Time	30 [year]
# nodes	51

The Fe(II) produced in equation 4, may also oxidize to form Fe(III) according to the following reaction:



The ratio of Fe(II), to Fe(III) is calculated based on the oxygen concentration present in the pore space and the pH of the pore water. The reaction products are added to the pore water at the point where they were produced, and are then transported using the advective-dispersive equation (Equation 6).

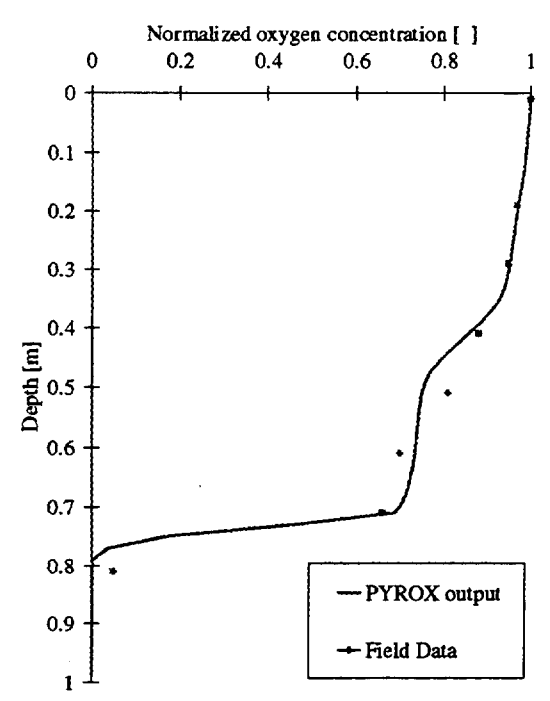


**Figure 3. Field and modelled oxygen concentrations from Nickel Rim mine-tailings impoundment, Sudbury, Ontario, piezometer nest location NR18. Field measurements made in June 1991 (8).**

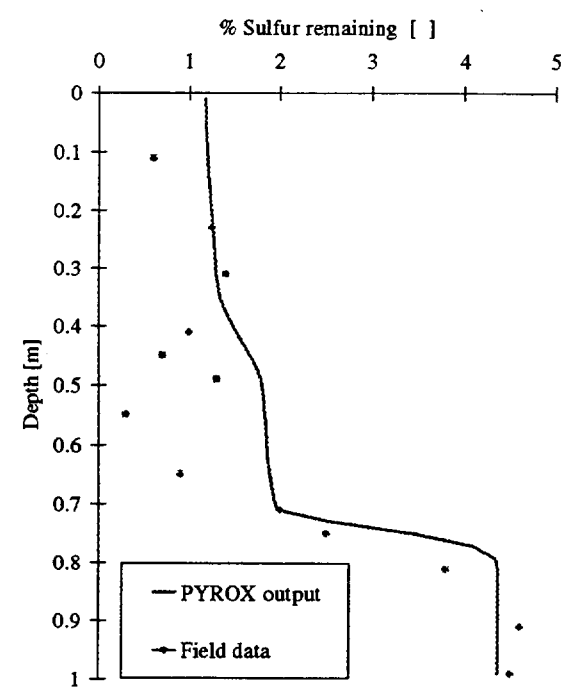


**Figure 4. Field and modelled sulfur concentrations from Nickel Rim mine-tailings impoundment, Sudbury, Ontario, piezometer nest location NR18. Field measurements made in June 1991 (8).**

$$\frac{\partial C_k}{\partial t} - \frac{\partial}{\partial x_i} \left( D_{ij} \frac{\partial C_k}{\partial x_j} \right) + \frac{\partial}{\partial x_i} (v_i C_k) - R_k = 0 \quad k = 1, \dots, N_c \quad (6)$$

where,

- $C_k$  - aqueous concentration of the component  $k$  [mol/kg]
- $D_{ij}$  - hydrodynamic dispersion tensor (see Bear (9)) [ $m^2/s$ ]
- $v_i$  - vector component of the average fluid velocity [m/s]
- $R_k$  - chemical source/sink term [mol/kg s]

All aqueous components in the simulation are transported separately using equation 6. The solid and aqueous chemistry is then equilibrated at each node in the domain, using the MINTEQA2 module. A description of MINTEQA2 can be found in Felmy et al. (10).

### One Dimensional Simulations

A one-dimensional column simulation was run based on data from the Nordic Main tailings impoundment near Elliot Lake, Ontario. The data was taken from Smyth (11), and Dubrovsky (12). The field location T3 was modelled because of the large unsaturated zone, and the abundance of data available at that location.

The Nordic Main tailings at Elliot Lake were deposited from 1957 to 1968. The tailings were treated with lime and limestone prior to deposition resulting in a pH of approximately 8. In 1972 additional lime and limestone were added to the surface of the tailings, along with fertilizer and sewage sludge as part of a revegetation program. Smyth (11) collected physical and chemical field data from the vadose zone of the tailings in 1980, and 1981, allowing for approximately 12 years of pyrite oxidation prior to collection of the data.

The column dimensions were 6.0 metres in length by 0.1 metres wide. The moisture content, porosity, bulk density, and pyrite content were used as input data for the PYROX (diffusion) module. Aqueous and available solid-phase data were used as input for the MINTRAN (reactive-transport) module. A steady state velocity of 0.62 m/a, based on the infiltration rate and the tailings porosity was used and is consistent with velocities calculated by Dubrovsky (12). Many of the solid-phase concentrations were not known and had to be inferred based on the conceptual model of the geochemical evolution of the Nordic uranium tailings developed by Smyth (11). The conceptual model includes a series of pH buffering mineral-dissolution reactions, including calcite, siderite, ferric hydroxide, and aluminum hydroxide. These minerals were included in the 1-D simulation as well as the mineral jarosite. Influx aqueous chemistry is loosely based on rain water composition from the area with modifications to account for chemicals added to the surface of the tailings during revegetation attempts. Tables 2 through 5 show influx chemistry, pore-water chemistry, solid-phase chemistry, and input diffusion parameters respectively. Table 6 lists the mineral phases included in the simulation and Table 7 lists the chemical species included in the simulation.

**Table 2. Influx chemistry for 1-D simulation.**

Aqueous Components	Concentration moles/litre
Ca <sup>2+</sup>	1.25e-2
Mg <sup>2+</sup>	1.04e-3
K <sup>+</sup>	9.00e-3
Cl <sup>-</sup>	1.14e-4
Al <sup>3+</sup>	1.28e-8
SO <sub>4</sub> <sup>2-</sup>	7.48e-3
Fe <sup>3+</sup>	2.32e-8
CO <sub>3</sub> <sup>2-</sup>	3.94e-3
H <sup>+</sup>	4.59e-3
Fe <sup>2+</sup>	5.36e-5
H <sub>4</sub> SiO <sub>4</sub>	1.99e-3

Selected results from the one-dimensional simulations are shown in Figure 1. The general trends observed in the modelled data correspond well with those of the field data. The pH profile shows a stepwise increase with depth where different mineral phases are acting as buffers. Near the surface, a jarosite buffered zone maintains the pH of the pore water at about 2. Below the jarosite zone is a ferrihydrite buffered zone where the pH is buffered at about 2.7. Gibbsite follows, buffering at a pH of around 3.7, followed by siderite at around 4.5, and finally calcite at a pH of about 5.9. Modelled aluminum concentrations match the field data very well with a spike in the concentration at a depth of about 1.6 m. The total iron concentrations show two distinct peaks. The upper peak in the ferrihydrite buffered zone, consists mostly of Fe(III), whereas the lower peak consists mostly of Fe(II). Below 3.0 meters discrepancies in the iron concentrations between modelled and field data are observed. These discrepancies may exist because the modelled results are based on the

**Table 3. Aqueous background chemistry for 1-D simulation.**

Aqueous Components	Concentration moles/litre
Ca <sup>2+</sup>	1.44e-2
Mg <sup>2+</sup>	2.30e-3
K <sup>+</sup>	6.00e-3
Cl <sup>-</sup>	1.14e-3
Al <sup>3+</sup>	2.59e-8
SO <sub>4</sub> <sup>2-</sup>	3.13e-2
Fe <sup>3+</sup>	1.48e-7
CO <sub>3</sub> <sup>2-</sup>	3.59e-2
H <sup>+</sup>	5.47e-2
Fe <sup>2+</sup>	5.39e-5
H <sub>4</sub> SiO <sub>4</sub>	1.91e-3

**Table 4. Solid background chemistry for 1-D simulation.**

Mineral Phase	Concentration moles/litre
Calcite	0.070
Lime	0.100
Gibbsite	0.045
Am. Silica	4.69E+1
Siderite	2.00E-2
Ferrihydrite	1.00E-6
Gypsum	0.174
Jarosite	0.0

**Table 5. Diffusion parameters for 1-D simulation.**

Diffusion Parameter	Value
D1	variable [m <sup>2</sup> /s]
D2	3.50 E-15 [m <sup>2</sup> /s]
Particle Radius	3.0 E-5 [m]
Porosity	variable
Bulk Density	variable [kg/m <sup>3</sup> ]
% Sulfur	1.61
Depth	6.0 [m]
Time	12.0 [year]
# nodes	121

**Table 6. Buffering reactions used in 1-D simulation.**

Mineral	Reaction	log K
Calcite	Ca <sup>2+</sup> + CO <sub>3</sub> <sup>2-</sup> ⇌ CaCO <sub>3</sub>	8.4789
Siderite	Fe <sup>2+</sup> + CO <sub>3</sub> <sup>2-</sup> ⇌ FeCO <sub>3</sub>	10.57
Gibbsite (c)	Al <sup>3+</sup> + 3H <sub>2</sub> O ⇌ Al(OH) <sub>3</sub> + 3H <sup>+</sup>	-8.11
Ferrihydrite	Fe <sup>3+</sup> + 3H <sub>2</sub> O ⇌ Fe(OH) <sub>3</sub> + 3H <sup>+</sup>	-4.891
Jarosite	K <sup>+</sup> + 3Fe <sup>3+</sup> + 2SO <sub>4</sub> <sup>2-</sup> + 6H <sub>2</sub> O ⇌ KFe <sub>3</sub> (SO <sub>4</sub> ) <sub>2</sub> (OH) <sub>6</sub> + 6H <sup>+</sup>	9.210

assumption that calcite is the buffering mineral below 3.0 m. Calcite was thought to be the mineral buffering the pore water in this zone because the pH remains constant and relatively high at a pH of around 5.9. In reality, it is unlikely that pure phase calcite will exist rather than some form of impure calcite as a solid solution. Another possible explanation for the discrepancies in the iron profile is that kinetic limitations may be preventing siderite from precipitating to equilibrium. Slow precipitation kinetics would cause iron to remain in solution longer, and thus the concentration observed would be higher than that calculated using an equilibrium approach. Some of the modelled solid phase concentration are shown in Figure 2. Unfortunately field determination of the concentrations of these mineral phases were not made.

## MINTOX Applications

The model is capable of 2-D simulations with oxygen diffusion occurring in one dimension. The most powerful application of the MINTOX model is in determining the effect of modifying physical or chemical properties of the tailings. Examples of this application would be to model the effects of adding moisture retaining covers, removing sulfide minerals from the tailings, or adding chemical components such as calcite to the shallow tailings. For example, simulations could be run to determine the most effective combination of cover properties such as thickness, moisture content, and porosity. Quantitative effects of limestone addition to the tailings prior to deposition could be assessed. The model could be used to determine the optimum quantity of limestone necessary to achieve neutralization of the acid which will be generated due to pyrite oxidation. Combinations of physical and chemical modifications can also be quantitatively assessed. Because of the high cost of preventative measures aimed at reducing acid-mine drainage, optimization of these preventative measures may result in large cost savings.

**Table 7. Species included in 1-D simulation.**

Reaction	$\Delta H_r^\circ$	log K
$H_2O \rightleftharpoons H^+ + OH^-$	13.345	-13.998
$H_4SiO_4^0 \rightleftharpoons H^+ + H_3SiO_4^-$	8.936	-9.929
$Mg^{2+} + CO_3^{2-} \rightleftharpoons MgCO_3^0$	2.535	2.981
$Mg^{2+} + CO_3^{2-} + H^+ \rightleftharpoons MgHCO_3^+$	-2.775	11.397
$Mg^{2+} + SO_4^{2-} \rightleftharpoons MgSO_4^0$	1.4	2.25
$Ca^{2+} + CO_3^{2-} + H^+ \rightleftharpoons CaHCO_3^+$	-0.869	11.453
$Ca^{2+} + CO_3^{2-} \rightleftharpoons CaCO_3^0$	3.547	3.225
$Ca^{2+} + SO_4^{2-} \rightleftharpoons CaSO_4^0$	1.47	2.309
$K^+ + SO_4^{2-} \rightleftharpoons KSO_4^-$	2.25	0.85
$Al^{3+} + 2H_2O \rightleftharpoons Al(OH)_2^+ + 2H^+$	0.0	-10.1
$Al^{3+} + 4H_2O \rightleftharpoons Al(OH)_4^- + 4H^+$	44.06	-23.0
$Al^{3+} + 3H_2O \rightleftharpoons Al(OH)_3^0 + 3H^+$	0.0	-16.0
$Fe^{2+} + H_2O \rightleftharpoons FeOH^+ + H^+$	13.2	-9.5
$Fe^{2+} + SO_4^{2-} \rightleftharpoons FeSO_4^0$	3.23	2.25
$CO_3^{2-} + H^+ \rightleftharpoons HCO_3^-$	-3.561	10.329
$CO_3^{2-} + 2H^+ \rightleftharpoons H_2CO_3^0$	-5.738	16.681
$Al^{3+} + H_2O \rightleftharpoons AlOH^{2+} + H^+$	11.90	-4.99
$Al^{3+} + SO_4^{2-} \rightleftharpoons AlSO_4^+$	2.15	3.02
$Al^{3+} + 2SO_4^{2-} \rightleftharpoons Al(SO_4)_2^-$	2.84	4.92
$H^+ + SO_4^{2-} \rightleftharpoons HSO_4^-$	4.91	1.987
$Fe^{3+} + H_2O \rightleftharpoons FeOH^{2+} + H^+$	10.399	-2.19
$Fe^{3+} + SO_4^{2-} \rightleftharpoons FeSO_4^+$	3.91	3.92
$Fe^{3+} + 2H_2O \rightleftharpoons Fe(OH)_2^+ + 2H^+$	0.0	-5.67
$Fe^{3+} + 3H_2O \rightleftharpoons Fe(OH)_3^0 + 3H^+$	0.0	-13.6
$Fe^{3+} + 2SO_4^{2-} \rightleftharpoons Fe(SO_4)_2^-$	4.6	5.42
$Fe^{3+} + e^- \rightleftharpoons Fe^{2+}$	-10.0	13.032
$CO_3^{2-} + 2H^+ \rightleftharpoons CO_{2(g)} + H_2O$	-0.53	18.16

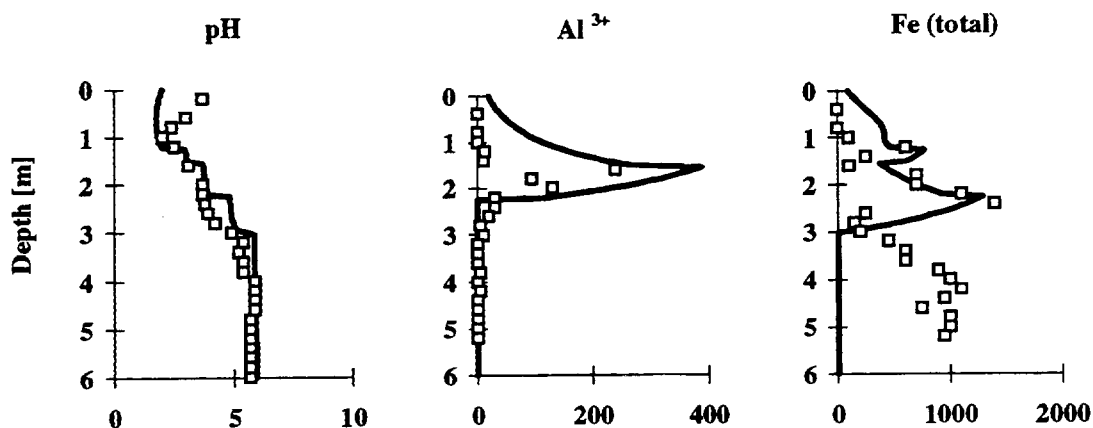


**Figure 1. Elliot Lake simulation results. Solid lines are MINTOX output, squares are field data from Smyth (10). Concentrations are in mg/l.**

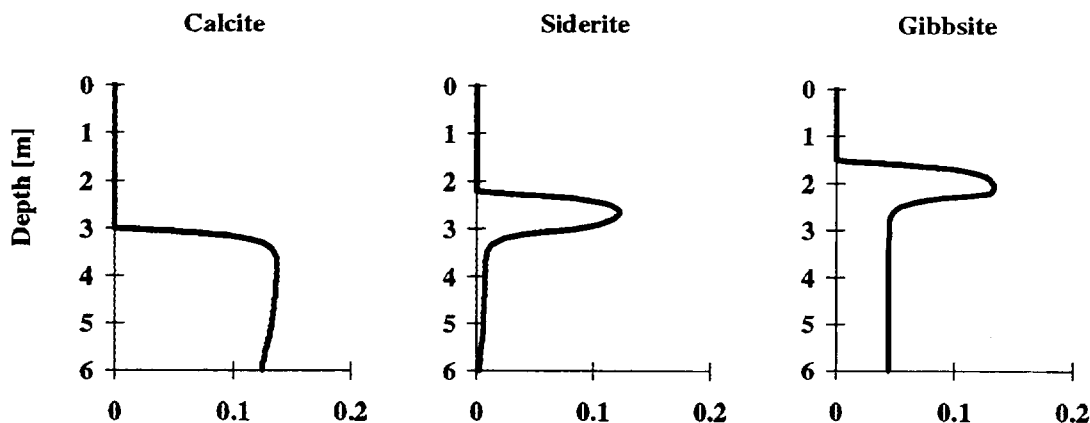


Figure 2. Elliot lake simulation results. Concentrations are in mol/l of solution.

### Conclusions

A numerical oxygen diffusion and pyrite oxidation model (PYROX) has been developed. The model is capable of modelling heterogeneous media where moisture content, porosity, pyrite content, and bulk density are variable with depth. The model can be used to determine rates of contaminant generation and the duration of pyrite oxidation. The effectiveness of oxygen diffusion barriers, such as moisture retaining covers, in reducing acid-mine drainage can be assessed. However, the model is not capable of determining the fate of the oxidation products once produced. Therefore, PYROX was coupled with the reactive transport model MINTRAN to produce the model MINTOX. MINTOX simulates the generation of oxidation products and the subsequent reactive transport of these oxidation products through the subsurface. Chemical reactions occurring between the pore water and the solid matrix are calculated, and thus the fate of the oxidation products may be determined. The effects of physical and chemical changes imposed on the tailings can be quantitatively assessed using MINTOX, and thus optimization of preventative measures can be assessed.

### References

1. Davis, G.B., and A.I.M. Ritchie. 1986. A model of oxidation in pyritic mine wastes: part 1: equations and approximate solution. *Applied Mathematical Modelling*, 10, 314-322.
2. Elberling, B., R.V. Nicholson, and J.M. Scharer. 1994. A combined kinetic and diffusion model for pyrite oxidation in tailings: a change in controls with time. *Journal of Hydrology*, 157, 47-60.
3. Walter, A.L., E.O. Frind, D.W. Blowes, C.J. Ptacek, and J.W. Molson. 1994. Modelling of multicomponent reactive transport in groundwater 1. Model development and evaluation. *Water Resources Research*, 30, (11), 3137-3148.
4. Davis, G.B. 1983. *Mathematical Modelling of Rate-Limiting Mechanisms of Pyrite Oxidation in Overburden Dumps*. Ph.D. Thesis. University of Wollongong. 159 p.
5. Davis, G.B., G. Doherty, and A.I.M. Ritchie. 1986. A model of oxidation in pyritic mine wastes: part 2: comparison of numerical and approximate solutions. *Applied Mathematical Modelling*, 10, 323-329.

6. Reardon, E.J., and P.M. Moddle. 1985. Gas diffusion coefficient measurements on uranium mill tailings: implications to cover layer design. *Uranium*, 2, 111-131.
7. Levenspiel, O. 1972. *Chemical Reaction Engineering*. John Wiley and Sons Inc., New York.
8. Johnson, H. R. 1993. *The Physical and Chemical Hydrogeology of the Nickel Rim Mine Tailings, Sudbury, Ontario*. M.Sc. Thesis. University of Waterloo. 108 p.
9. Bear, J. 1972. *Dynamics of Fluids in Porous Media*. American Elsevier Publishing Company, Inc., New York, N.Y., 764 p.
10. Felmy, A.R., D.C. Girvin, and E.A. Jenne. 1983. *MINTEQ: A Computer Program for Calculating Aqueous Geochemical Equilibria*. Report, U.S. Environmental Protection Agency, Washington D.C., 62 p.
11. Smyth, D. J. A. 1981. *Hydrogeological and Geochemical Studies Above the Water Table in an Inactive Uranium Tailings Impoundment Near Elliot Lake, Ontario*. M.Sc. Project. University of Waterloo. 72 p.
12. Dubrovsky, N.M. 1986. *Geochemical Evolution of Inactive Pyritic Tailings in the Elliot Lake Uranium District*. Ph.D. Thesis. University of Waterloo. 373 p.